# Smart Distribution System Operations with Price-Responsive and Controllable Loads

Isha Sharma, *Student Member, IEEE,* Kankar Bhattacharya, *Senior Member, IEEE,* and Claudio Cañizares, *Fellow, IEEE*

***Abstract*—This paper presents a new modeling framework for analysis of impact and scheduling of price-responsive as well as controllable loads in a three-phase unbalanced distribution system. The price-responsive loads are assumed to be linearly or exponentially dependent on price, i.e., demand reduces as price increases and vice versa. The effect of such uncontrolled price-responsive loads on the distribution feeder is studied, as customers seek to reduce their energy cost. Secondly, a novel constant energy load model, which is controllable by the Local Distribution Company (LDC), is proposed in the paper. A controllable load is one which can be scheduled by the LDC through remote signals, demand response programs or through customer-end home energy management systems. Minimization of cost of energy drawn by LDC, feeder losses, and customers cost pertaining to the controllable component of the load, are considered as objectives from the LDC's and customers' perspective. The effect of a peak demand constraint on the controllability of the load is further examined. The proposed models are tested on two feeders: the IEEE 13-node test feeder and a practical LDC feeder system. Detailed studies examine the operational aspects of price-responsive and controllable loads on the overall system. It is observed that the LDC controlled load model results in a more uniform system load profile, and that with a reduction in the peak demand cap, the energy drawn decreases, consequently reducing feeder losses and LDC's and customers' costs.**

***Index Terms*—Demand response, price-responsive loads, three-phase unbalanced distribution system, optimal feeder operation.**

## I. Nomenclature

| | |
|---|---|
| *Indices* | |
| $C$ | Controllable capacitor banks. |
| $C_n$ | Controllable capacitor banks at node $n$. |
| $k$ | Hours, $k$=1,2,...,24. |
| $l$ | Series elements. |
| $L$ | Loads. |
| $L_n$ | Loads at node $n$. |
| $n$ | Nodes. |
| $p$ | Phases, $p$=$a, b, c$. |
| $r$ | Receiving-end. |
| $r_n$ | Receiving-ends connected at node $n$. |
| $s$ | Sending-end. |
| $s_n$ | Sending-ends connected at node $n$. |
| $SS$ | Substation node. |
| $t$ | Controllable tap changers. |
| *Parameters* | |
| $\alpha$ | Share of price-responsive load [p.u.]. |
| $\alpha_1$ | Share of controllable/dispatchable loads [p.u.]. |
| $\beta_1, \beta_2$ | Customer defined constants [p.u.]. |
| $\varphi$ | LDC defined peak demand cap [p.u.]. |
| $\gamma$ | Decay rate of demand with price [kWh/$]. |
| $\theta$ | Load power factor angle [rad]. |
| $\Delta S$ | Percentage voltage change for each LTC tap. |
| $\Delta Q$ | Size of each capacitor block in capacitor banks [VAr]. |
| $\rho$ | Electricity price [$/kWh]. |
| $\rho_1$ | Retail electricity price [$/kWh]. |
| $\rho_{max}, \rho_{min}$ | Maximum and minimum energy price [$/kWh]. |
| $A, B, C, D$ | Three-phase ABCD parameter matrices. |
| $Io$ | Load phase current at nominal values [A]. |
| $I^{max}$ | Maximum feeder current limit [A]. |
| $m$ | Slope of a linear price-responsive demand function. |
| $\overline{N}$ | Maximum number of capacitor blocks available. |
| $P^{max}$ | Maximum demand [W]. |
| $PD$ | Total load profile [W]. |
| $PD^o, PD^{Cr}$ | Given, critical real power load [W]. |
| $PD^{Exp}$ | Exponential price-responsive real power load [W]. |
| $PD^{Lin}$ | Linear price-responsive real power load [W]. |
| $\overline{PD}, \underline{PD}$ | Maximum and minimum real power demand [W]. |
| $QD^o$ | Given reactive power load [VAr]. |
| $QD^{Fx}$ | Fixed reactive power load [VAr]. |
| $\overline{T}, \underline{T}$ | Maximum and minimum tap changer position. |
| $V^o$ | Specified nominal voltage [V]. |
| $Vmax, Vmin$ | Maximum and minimum voltage limit [V]. |
| $X$ | Reactance of capacitor [Ω]. |
| $Z$ | Load impedance at nominal values [Ω]. |
| *Variables* | |
| $cap$ | Number of blocks of switched capacitor banks. |
| $I'$ | Current supplying the variable demand [A]. |
| $I$ | Current phasor [A]. |
| $\overline{I}$ | Vector of three-phase line current phasors [A]. |
| $J_1, J_2, J_3$ | Objective functions. |
| $P'$ | Real power of controllable loads [W]. |
| $Q$ | Reactive power of capacitor banks [VAr]. |
| $Q'$ | Reactive power of controllable loads [VAr]. |
| $T$ | Tap position. |
| $V$ | Voltage phasor [V]. |
| $\overline{V}$ | Vector of three-phase line voltages [V]. |

This work was supported by the Ontario Centres of Excellence (OCE), Hydro One Networks Inc., Milton Hydro Distribution Inc., Energent Inc., and the Ontario Power Authority (OPA).

Isha Sharma (i4sharma@uwaterloo.ca), Kankar Bhattacharya (kankar@uwaterloo.ca) and Claudio Cañizares (ccanizares@uwaterloo.ca) are with the Department of Electrical and Computer Engineering, University of Waterloo, Waterloo, Canada.

## II. INTRODUCTION

LOCAL Distribution Companies (LDCs) are gradually integrating advanced technologies and intelligent infrastructure to maximize distribution system capability, modernize the grid, and lay the foundation for smart homes. Significant efforts are being made to integrate intelligent control algorithms with information technology to manage energy consumption and thereby regulate load growth. Demand Response (DR) programs are being implemented by utilities and LDCs to alter the load shape in response to price signals or operator requests during critical conditions. DR is defined by FERC in [1] as: "Changes in electricity use by demand-side resources from their normal consumption patterns in response to changes in the price of electricity, or to incentive payments designed to induce lower electricity use at time of high wholesale market price or when system reliability is jeopardized." There are two different categories of DR programs, identified in [1]: one is time-based which includes time-of-use (TOU) pricing, real-time pricing (RTP), critical peak pricing with/without control, etc.; and the second is incentive-based such as direct load control (DLC), demand side bidding and buyback, emergency demand response, non-spinning reserves, regulation service, and interruptible load. These programs help the LDC to maintain a fairly uniform load level, thereby reducing its need for new supply resources or feeders.

Although DR has taken center-stage in the context of smart grids, load/demand side management (DSM) programs have been in existence and practice for several decades now [2]. For example, the early work in this topic [3] presents the basic philosophy in which the generation and demand respond to each other in a cooperative fashion and are in a state of continuous equilibrium. The authors propose that one way to reduce costs is to use direct utility-consumer communications to implement a "load follow supply" concept. Under such a system, the customer's demand would be controlled through interruption of power for specific uses.

Various incentive rate designs have been implemented in the past by US utilities, of which the most common have been interruptible tariffs and TOU pricing [4]. After deregulation of the electricity sector, load control and DSM programs have been implemented in several electricity markets and have provided various types of ancillary services such as supplemental reserve services [5]. In the research literature, various formulations for utility-customer interaction and price elasticity of demand have been reported. Thus, in [6], an integrated customer response model combined with price forecasting has been developed; the system demand is decomposed into statistically uncorrelated categories and separate cross-time elasticity matrices for each category are proposed, and actual demand data from Hong Kong's China Light & Power Company is processed to decompose the load data and develop the models. Customer response to spot price difference is modeled in [7], using linear and exponential functions to determine real-time interruptible tariffs. Customers' behavior is modeled using a matrix of self- and cross-elasticity in [8], considering generation scheduling and wholesale market clearing; a typical price-demand curve, where the demand exponentially increases when the price decreases, is discussed, and the structure of an elasticity matrix for various types of customer reactions such as anticipating customer, flexible customer, inflexible customer, etc., is presented, stating that the price-demand relationships can be linearized for the sake of simplification of the computations without any significant loss of generality.

In [9], the impact of demand side price-responsiveness on the oligopoly market performance is examined considering exogenous changes in self elasticity; a linear relationship between customer demand and market price is formulated considering different degrees of price-responsiveness. Incentive-based DR programs such as interruptible/curtailable loads are modeled in [10], based on price elasticity of demand and quadratic customer benefit function in the context of transmission systems, the proposed model improves the load shape, load level, and benefits customers. In [11], a security constrained unit commitment (SCUC) problem with price responsive loads is presented and DR is represented by bid curves which are submitted for market clearing; in this context, the responsive loads can be curtailed or shifted in time. In [12], an economic model of responsive loads is proposed based on price elasticity of demand and customers benefit function which is implemented in a cost-emission based Unit Commitment (UC) problem. In another UC model considering wind resources, demand shifting and peak shaving decisions are determined considering customers' elasticity [13], resulting in reduced generation cost and demand peaks. In a similar UC model in [14], a critical peak pricing with load control model that can assist the realization of DR programs is proposed. DR methodologies are proposed in [15] to integrate short-term responsiveness of demand into a generation technology mix optimization model; loads are shifted across hours using self- and cross-elasticity in response to price changes, and elastic demand functions are built using historic hourly demand levels and assumed levels of elasticity. In a recent work [16], load profiles have been estimated using survey data and questionnaires for a large cross-section of residential customers in Finland, studying the impact of DR on distribution system operations.

Research has been reported in recent literature on smart load management at the customer end. The optimal operation of six dc smart houses with controllable loads connected to a power system is reported in [17]. The objective is to minimize the interconnection point power flow (power flow from system to smart grid) fluctuations, and the problem is solved using Tabu Search. In [18], a multi-objective optimization model is proposed for selection of load control strategies. A linear programming (LP) model to optimize the system peak load through DLC programs in residential, commercial and industrial sectors is presented in [19]. A pilot study in Norway reported in [20] examines the potential for DR through incentives, hourly spot pricing, and reminding customers of peak price hours using smart meter and remote load control. An LP model maximizing the utility function of a customer is proposed in [21], that considers RTP to adjust the customers hourly load. A DR strategy, targeted at the household level taking into consideration customer preferences, choice of

comfort level and load priority, is proposed in [22]. In [23], a comprehensive mathematical optimization model is proposed for residential energy hubs to optimally control residential appliances while keeping in mind the customer preferences and comfort.

A decision-making framework for LDCs considering a three-phase unbalanced distribution system with comprehensive detail of system components, is proposed in [24]. The proposed Distribution Optimal Power Flow (DOPF) operating objective simultaneously considers the minimization of total energy drawn by LDC and switching operations of Load Tap Changers (LTCs) and capacitors. However, the proposed DOPF framework considers the loads to be fixed, which, in the context of smart grids, may not always be so. Customers are increasingly being equipped with in-house energy management systems that schedule appliance operations according to their preferences. Many customers are now price-responsive, because of the introduction of smart meters and TOU and RTP tariffs, reducing their demand when price is high, and vice versa. The price-responsiveness of customers can be attributed to different types of loads, such as critical loads, interruptible loads and deferrable loads [25]. Critical loads are those that cannot be shifted or shed at any time, interruptible loads can be curtailed if needed and deferrable loads can be shifted to latter hours, if required.

Based on the aforementioned review of existing technical literature, this paper considers for the first time two categories of loads, price-responsive and LDC controlled loads, to study the operational aspects of unbalanced distribution systems in the context of a proposed DOPF. It is envisaged that in a smart grid environment, customers will be privy to pricing information and their loads would respond to LDC control signals or be scheduled by the customer considering its own priorities. The first category of load models proposed in this paper are price-responsive loads, which considers a parametric (linear and exponential) representation of the load as a function of the RTP, wherein as price increases the load decreases, assuming a rational behavior of customers. Secondly, a novel constant energy load model is proposed, controllable by the LDC, representing critical and deferrable loads.

The main contributions of this paper can be summarized as follows:

- While several authors have incorporated price-responsive loads in power system operations, as discussed earlier, this is the first attempt where such loads are being considered in an unbalanced distribution system at the retail customer level, for the purpose of optimal feeder operation.
- The price-responsive load models in parametric form characterize the customers' behavior at each load node and phase, with respect to prices.
- A new mathematical model is proposed to represent controllable or dispatchable loads on an unbalanced distribution feeder. These loads are assumed to receive control/dispatch signals from the LDC and alter their energy usage patterns as per its operating objectives, thus allowing the LDC to indirectly achieve direct load control in the context of DR programs.
- The proposed price-responsive and controllable/dispatchable loads, or smart loads, are integrated within a DOPF model to examine their impact on distribution system operation. Various scenarios, including uncertainty in model estimation, are constructed to study the system impact of differing operating perspectives of the LDC and the customers.

One key feature of smart grids is automation technology that is envisaged to enable the LDCs to control/dispatch customer appliances from a central location [26]. Thus, the proposed framework is based on smart loads that control/dispatch appliances and participate in DR programs to bring about improved operational efficiency in the distribution grid, considering that two-way communication infrastructures can facilitate the interaction of loads with distribution feeder or LDC.

The rest of the paper is organized as follows: Section III presents the mathematical models of the unbalanced distribution system, price-responsive loads and controllable loads. Section IV describes the proposed DOPF model of the three-phase distribution system that includes the price-responsive loads and controlled loads with different objective functions. Section V first presents a description of the IEEE 13-node test feeder and a practical LDC feeder, and the associated assumptions made for the analysis; it then presents and discusses the results obtained from various case studies carried out on these test feeders. Section VI highlights the main conclusions and contributions of the presented research.

## III. Mathematical Modeling Framework

### A. Distribution Systems [24], [27]

A generic distribution system comprises series and shunt components, the series components include conductors/cables, transformers, LTCs and switches, which are modeled in this work using ABCD parameters. The ABCD parameters define the relationship between the sending-end and the receiving-end nodes and can be computed as [27]:

$$\begin{bmatrix} \overline{V}_{s,p,k} \\ \overline{I}_{s,p,k} \end{bmatrix} = \begin{bmatrix} A_{(l\times p)} & B_{(l\times p)} \\ C_{(l\times p)} & D_{(l\times p)} \end{bmatrix} \begin{bmatrix} \overline{V}_{r,p,k} \\ \overline{I}_{r,p,k} \end{bmatrix} \qquad \forall l, \forall p, \forall k \tag{1}$$

where all variables and parameters for this and other equations are properly defined in Section I. The ABCD parameters for conductors, cables, transformers and switches are constants. Switches are represented as zero impedances, conductors and cables as $\pi$-equivalent circuits, and three-phase transformers are modeled based on the type of connection (wye or delta). Voltage regulating transformers in a distribution system are equipped with LTCs, whose ABCD parameters depend on the tap position at a given time $k$. Thus, B and C are null matrices while the A and D matrices of the LTCs are modeled using the following equations:

$$A_{t,k} = \begin{bmatrix} 1 + T_{t,a,k}\,\Delta S & 0 & 0 \\ 0 & 1 + T_{t,b,k}\,\Delta S & 0 \\ 0 & 0 & 1 + T_{t,c,k}\,\Delta S \end{bmatrix} \tag{2}$$

$$D_{(t\times k)} = A^{-1}_{(t\times k)} \qquad \forall t, \forall p, \forall k \tag{3}$$

where the tap controls in the respective phases for the LTCs are considered continuous variables to simplify the analysis, but without loss of generality, and are assumed to take any value between -16 and +16, for a 32-step LTC.

Shunt components comprise loads and capacitor banks and are modeled as constant impedance loads. The following equation represents wye-connected impedance loads on a per-phase basis:

$$V_{L,p,k} = Z_{L,p,k} I_{L,p,k} \qquad \forall L, \forall p, \forall k \qquad (4)$$

Capacitor banks are modeled as multiple capacitor blocks with switching options, on a per-phase basis, as follows:

$$V_{C,p,k} = X_{C,p,k} I_{C,p,k} \qquad \forall C, \forall p, \forall k \qquad (5)$$

$$jX_{C,p,k} = j\frac{V^{o2}_{C,p,k}}{Q_{C,p,k}} \qquad \forall C, \forall p, \forall k \qquad (6)$$

$$Q_{C,p,k} = cap_{C,p,k}\ \Delta Q_{C,p,k} \qquad \forall C, \forall p, \forall k \qquad (7)$$

where $cap_{C,p,k}$ is assumed to be continuous variables to simplify the analysis, but without loss of generality, and can take any positive value from 0 to $\overline{N}_{C,p}$.

To model the distribution system in its totality, these elements are required to satisfy the current balance at each node and phase:

$$\sum_{l} I_{l,p,k}(\forall r_n) = \sum_{l} I_{l,p,k}(\forall s_n) + \sum_{L} I_{L_n,p,k} + \sum_{C} I_{C_n,p,k} \qquad \forall n, \forall p, \forall k \qquad (8)$$

Furthermore, the voltage at the node and phase at which a given set of components are connected is the same as the corresponding nodal voltages:

$$V_{l,p,k}(\forall s_n) = V_{l,p,k}(\forall r_n) = V_{L_n,p,k} = V_{C_n,p,k} \qquad \forall n, \forall p, \forall k \qquad (9)$$

### B. Uncontrolled Price-Responsive Loads

An overview of the proposed smart distribution system operational framework with uncontrolled price-responsive loads is presented in Fig. 1. It is assumed that customers would be equipped with Home Energy Management Systems (HEMS) [23], based on which they respond to price $\rho_k$ by adjusting their consumption $PD_k(\rho_k)$. Two different price-demand relationships namely, linear and exponential, are considered for the studies. The reason for choosing the linear model is its simplicity in representing the price-demand relationship, while the exponential model is chosen since it represents a typical nonlinear price-demand relationship [7]- [9]. The price-responsiveness of customers can effectively be determined in real-life through historical data of price and load demand, or using a thorough customer survey; hence the parameters of the proposed models can be estimated using historical data sets.

In Fig. 1, it is also assumed that the LDC would be equipped with a Smart Load Estimator (SLE), which receives real-time load consumption data from customers' smart meters to develop price-responsive models for the loads. These price-responsive load models, estimated by the SLE, would be used

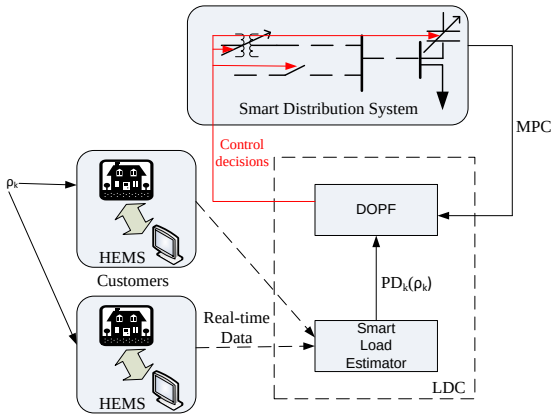


Fig. 1. Smart distribution system with uncontrollable price-responsive loads.

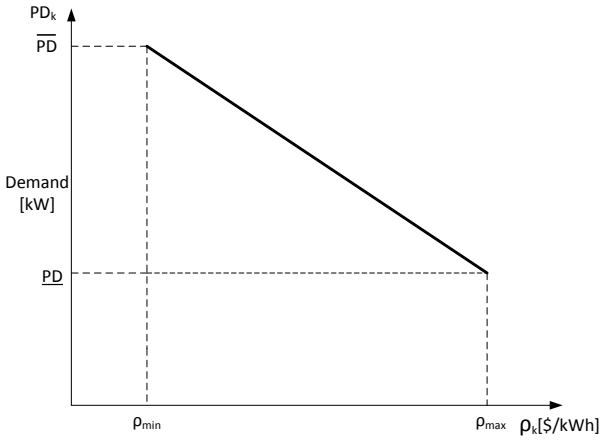


Fig. 2. Linear relation between demand and electricity price.

as an input by the LDC for real-time smart distribution system operation through the proposed DOPF to optimally control the distribution feeder using a Model Predictive Control (MPC) approach [28]. Thus, the proposed model would be executed based on the frequency of the incoming real-time data, which could be every 5, 10 or 15 minutes to take care of the changes in the system parameters, particularly load demand, which can change dynamically. Furthermore, it is assumed that some fraction of the loads would respond to electricity prices by increasing or decreasing their consumption as per their convenience, or behaving as deferrable loads, while the rest is considered to be fixed or critical loads.

*1) Linear Price-Responsive Load Model:* In this case, the customers respond to electricity price increase by reducing the consumption linearly as RTP increases, and vice versa. Figure 2 shows the demand variation of the price-responsive component. The 24-hour load profile considering fixed (critical) and linear price-responsive components is given by:

$$PD_{L,p,k} = PD^{Cr}_{L,p,k} + PD^{Lin}_{L,p,k} \qquad \forall L, \forall p, \forall k \qquad (10)$$

The 24-hour load profile for the real and reactive components for the fixed component of the load is given by:

$$\begin{cases} PD^{Cr}_{L,p,k} = (1-\alpha) PD^{o}_{L,p,k} & \forall L, \forall p, \forall k \\ QD^{Cr}_{L,p,k} = (1-\alpha) QD^{o}_{L,p,k} & \forall L, \forall p, \forall k \end{cases} \qquad (11)$$

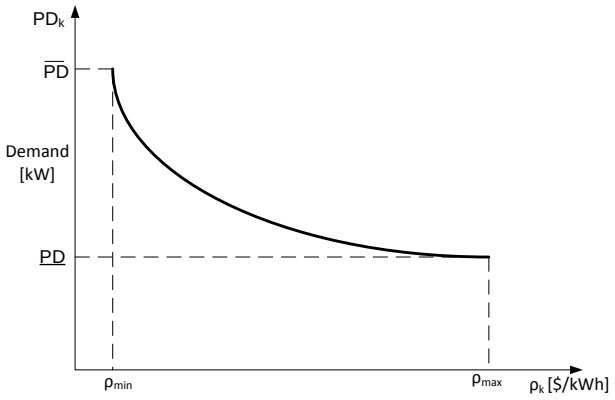


Fig. 3. Exponential relation between demand and electricity price.

where $\alpha$ is the fraction of load that can be deferred or interrupted. Similarly, the 24-hour load profile for the price-responsive component of load (Fig. 2) can be represented as:

$$PD^{Lin}_{L,p,k} = \begin{cases} m_{L,p,k}(\rho_k - \rho_{min}) + \overline{PD}_{L,p,k} & \rho_{min} < \rho_k < \rho_{max} \\ \overline{PD}_{L,p,k} & \rho_k \leq \rho_{min} \\ \underline{PD}_{L,p,k} & \rho_k \geq \rho_{max} \end{cases} \tag{12}$$

where

$$\begin{aligned} m_{L,p,k} =& \frac{\underline{PD}_{L,p,k} - \overline{PD}_{L,p,k}}{\rho_{max} - \rho_{min}} && \forall L, \forall p, \forall k \\ \overline{PD}_{L,p,k} =& \beta_1 \alpha PD^o_{L,p,k} && \forall L, \forall p, \forall k \\ \underline{PD}_{L,p,k} =& \beta_2 \alpha PD^o_{L,p,k} && \forall L, \forall p, \forall k \end{aligned} \tag{13}$$

In (13), $m$ represents the slope of the line, and is always negative. As per (12), when the price lies in the range $\rho_{min} < \rho_k < \rho_{max}$, there is a reduction in demand; when $\rho_k \leq \rho_{min}$, the price-responsive demand component is capped at $\overline{PD}$, while for $\rho_k \geq \rho_{max}$, this component is fixed at $\underline{PD}$. The parameters $\rho_{max}$, $\rho_{min}$, $\beta_1$ and $\beta_2$ represent the customers' characteristics and reflect the impact of the energy prices on the demand. It should be noted that the reactive power consumption of the linear price-responsive component of the loads $QD^{Lin}$ is obtained from (13) considering a fixed power factor.

*2) Exponential Price-Responsive Load Model:* In this case, the customers respond to electricity price increase by reducing the consumption exponentially as RTP increases, and vice versa. Figure 3 shows the demand variation with respect to the RTP for the exponentially price-responsive and the fixed component of the loads, which yield the 24-hour load profile as follows:

$$PD_{L,p,k} = PD^{Cr}_{L,p,k} + PD^{Exp}_{L,p,k} \quad \forall L, \forall p, \forall k \tag{14}$$

The fixed component of the load profile is similar to that discussed in (11) while the exponential component is given by:

$$PD^{Exp}_{L,p,k} = \begin{cases} \overline{PD} e^{-\gamma(\rho_k - \rho_{min})} & \rho_{min} < \rho_k < \rho_{max} \\ \overline{PD}_{L,p,k} & \rho_k \leq \rho_{min} \\ \underline{PD}_{L,p,k} & \rho_k \geq \rho_{max} \end{cases} \tag{15}$$

where $\gamma$ represents the customers' sensitivity to energy prices, i.e., the decay rate of the demand with respect to price. As per (15), when the price lies in the range $\rho_{min} < \rho_k < \rho_{max}$, it results in a reduction in demand; when $\rho_k \leq \rho_{min}$, the price-responsive demand component is capped at $\overline{PD}$, while for $\rho_k \geq \rho_{max}$, this component is fixed at $\underline{PD}$. As in the previous model, the load power factor is assumed constant in both components of the load.

Apart from the linear and exponential models, other price-responsive load models, such as a price-elasticity matrix [29], could be used to represent uncontrolled price-responsive loads. However, since the main thrust of the paper is to compare controllable and uncontrollable loads, such models would only affect the a-priori load profiles of uncontrolled price-responsive loads, having limited impact on the main results and conclusions, and are hence not considered here.

### C. LDC Controlled Loads

Figure 4 presents the operational framework for the LDC with controllable loads. With the introduction of RTP or TOU tariffs, there is a possibility that customers would tend to shift their demand by scheduling their appliance usage, as much as possible, to times when the electricity prices are low. However, such demand shifts may create unwarranted new peaks in the distribution feeder. In order to alleviate this problem in the proposed framework, it is envisaged that the LDC will send control/dispatch signals to individual customers, $k$, while also determining optimal decisions on its feeder operating variables such as taps and capacitor switching. The loads which respond to the LDC's operating objective and can be shifted across intervals, while keeping the energy consumption of the customer constant over a day, play an important role in smoothening the system load profile. In this case, there is a need to ensure that no new peaks are created while shifting the controllable loads across intervals. Hence, the LDC defines a peak demand cap $\overline{PD}_k$ for the system, considering grid constraints and operating limits at any interval, and schedules the controllable loads accordingly. The proposed DOPF, considering objective functions from the perspective of the LDC and customers, would provide the required smart operating decisions. This category of load models considers deferrable loads which cannot be interrupted but can be shifted to other hours, thus ensuring the same energy consumption from the customer over the day.

The fixed or critical component of the load is modeled as in (4), while the controllable component of the load is modeled as:

$$|I^{'}_{L,p,k}|(\angle V_{L,p,k} - \angle I^{'}_{L,p,k}) = |Io_{L,p,k}|\angle\theta_{L,p,k} \quad \forall L, \forall p, \forall k \tag{16}$$

$$V_{L,p,k} I^{'*}_{L,p,k} = P^{'}_{L,p,k} + jQ^{'}_{L,p,k} \quad \forall L, \forall p, \forall k \tag{17}$$

In order to ensure that there is no change in the total daily energy consumption, so that the load is only shifted over the day, the following constraint is needed:

$$\sum_k P^{'}_{L,p,k} + (1 - \alpha_1) \sum_k PD^o_{L,p,k} = \sum_k PD^o_{L,p,k} \; \forall L, \forall p \tag{18}$$

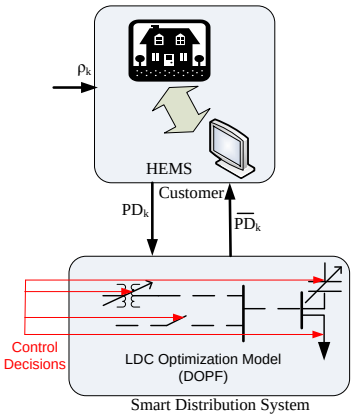


Fig. 4. Smart distribution system with controllable loads.

With this constraint, there is a possibility that significant amounts of load are shifted to certain specific hours, resulting in a new peak in the system. In order to ensure that no such new peak is created, an additional constraint is added:

$$P^{'}_{L,p,k} + (1-\alpha_1)PD^{o}_{L,p,k} \leq \varphi P^{max}_{L,p,k} \quad \forall L, \forall p, \forall k \tag{19}$$

where $\varphi$ determines the peak demand cap enforced by the LDC to maintain system conditions within acceptable operating limits.

To include this load model in the DOPF, (8) is modified by considering the load current of the constant energy model as follows:

$$\sum_{l} I_{l,p,k}(\forall r_n) = \sum_{l} I_{l,p,k}(\forall s_n) + \sum_{L} I_{L_n,p,k} + \sum_{C} I_{C_n,p,k} + \sum_{L} I^{'}_{L_n,p,k} \quad \forall n, \forall p, \forall k \tag{20}$$

## IV. Smart Distribution System Operations

The three-phase DOPF model determines feeder operating decisions for various objective functions considering grid operational constraints for both price-responsive and LDC controlled loads. The objective functions are formulated either from the perspective of the LDC or that of the customers, as follows:

- Minimize the total cost of energy drawn by the LDC from the external grid over a day:

$$J_1 = \sum_{k} \left( \sum_{n} \sum_{p} Re\left( V_{SS_{k,n,p}} I^{*}_{SS_{k,n,p}} \right) * \rho(k) \right) \tag{21}$$

This objective assumes that the LDC purchases energy from the external electricity market at the prevailing hourly prices. The LDC can either be a retailer or a Distribution Company (DISCO); in this paper, the LDC is assumed to be a DISCO that has network operations responsibilities only. Although profit maximization would ideally be an appropriate objective to represent the LDC's interest, the retail price of energy ($\rho_1$) at which it sells electricity to customers will be regulated by a regulator, and can be represented as:

$$\rho_1(k) = \rho(k) + \text{a posteriori constant factor} \tag{22}$$

where the constant factor depends on the LDCs network costs, global adjustments, etc., which are not known a priori. In the absence of such information, maximization of LDC's profit is not possible in the present framework; hence, the LDC cost of energy drawn $J_1$ is minimized instead. On the other hand, if the LDC is a retailer, then competition in retail and wholesale markets will determine the retail price, and accordingly a profit function would be maximized, which is a particular issue beyond the scope of this paper.

- Minimize total feeder loss over a day:

$$J_2 = \sum_{k} \sum_{n} \sum_{p} Re\left( V_{k,n,p} I^{*}_{s_{k,n,p}} - V_{k,n,p} I^{*}_{r_{k,n,p}} \right) \tag{23}$$

Since loads are considered to be voltage dependent, this objective seeks to improve the voltage profile across distribution nodes.

- Minimize the energy cost of customers with controllable loads:

$$J_3 = \sum_{k} \left( \sum_{n} \sum_{p} P'_{k,n,p} \right) \rho_1(k) \tag{24}$$

This objective is formulated from the perspective of the customer, and can be used by the LDC to study the system impact of controllable smart loads, which typically seek to minimize their energy costs. It is assumed that all customer homes are equipped with smart meters and are subject to RTP or TOU tariff $\rho_1(k)$, and that customers have sufficient information or smart load controls to schedule their appliances accordingly. In real life, the retail price $\rho_1(k)$ is not the same as $\rho(k)$ because $\rho_1(k)$ should include the LDC network costs, global adjustments, etc. In the absence of knowledge on retail electricity prices, and since retail pricing is beyond the scope of this paper, for minimization of $J_3$, a simple assumption is made that $\rho_1(k) = \rho(k)$.

It should be mentioned that in traditional interruptible load management problems, a cost of load curtailment is usually considered in the objective function [7]. However, in this work such a cost has not been considered for reasons, as explained below:

- Price-responsive Loads: In this case, the entire demand is considered to be parametric, and thus the change in demand to price variations is calculated exogenously, based on the pre-defined linear or exponential functions, which are then input to the proposed DOPF. Thus, the DR is not a variable but known a priori to the LDC (as given), and hence there is no need to consider the cost of load shifting in the objective function $J_1$.
- Controllable Loads: In this case, the controllable component is modeled as a variable in the proposed DOPF, with (18) ensuring that the total energy consumption remains constant over the day. Since the cost of load shifting is not being considered, it may happen that the entire controllable component of load could be shifted out from an hour to another hour, which is acceptable since the customer has already declared to the LDC the amount

of load that is shiftable and thus controllable. Another possibility is that the variable component of the load at any given time may be zero, if no cost is attached to it. This behavior is expected in DR programs that have one-time incentives as opposed to incentives based on operations. For example, some programs have in-kind incentives such as a free installation of thermostats or vouchers, in which one cannot consider a cost of load curtailment, as is the case of the peaksaver PLUS® Program in Ontario [30], implemented by the LDCs in the province, in which there is no direct payment to customers for controlling their loads. Since from the distribution feeder operational point of view, this model represents the extremes of load shifting, no costs were assumed here. However, the cost of load curtailment could be included in the proposed DOPF by adding a cost term associated with load shifting energy to $J_1$ in (21).

The operating constraints on voltage, feeder current, tap operation and capacitor switching are imposed, as follows:

$$V^{min} \leq |V_{n,p,k}| \leq V^{max} \qquad \forall n, \forall p, \forall k \tag{25}$$

$$|I_{i,j,p,k}| \leq I_{i,j}^{max} \qquad \forall i \in s_n, \forall j \in r_n, \forall p, \forall k \tag{26}$$

$$\underline{T}_{t,p} \leq T_{t,p,k} \leq \overline{T}_{t,p} \qquad \forall t, \forall p, \forall k \tag{27}$$

$$0 \leq cap_{C,p,k} \leq \overline{N}_{C,p} \qquad \forall C, \forall p, \forall k \tag{28}$$

It should be mentioned that the proposed DOPF is somewhat similar to reliability-based DR programs, however, the present study applies to the distribution feeder level, and hence the model formulated is not the traditional security constrained power flow or OPF, but a DOPF. In this context, using the proposed DOPF with controllable loads can bring about significant modifications to the LDC's load curve and thus affect system reliability, especially considering peak demand constraints, that directly affect the overall reliability of the system, at all voltage levels. Observe that the DOPF considers each component of the distribution feeder such as the transformers, cables, switches, and loads at each node and phase, representing loads in a variety of ways. This results in a rather complex, and challenging optimization problem, as compared to the traditional reliability-based DR programs. In this case, the objective function (min. costs and losses) represent the LDC's "normal" operational perspective, and thus the model seeks to examine how DR programs will affect the distribution feeder (not the transmission system) operation. Thus, the proposed approach is different from the traditional, transmission system view and analysis of DR programs, rather concentrating on the impact and applications of these programs to distribution feeders and LDC operators.

The main purpose of the paper is to study the impact of price-responsive and controllable loads on the feeder, and not their optimal voltage control; taps and capacitors are modeled as continuous variables to avoid introducing integer variables, thus resulting in a Non-Linear Programming (NLP) DOPF model, which is computationally manageable. In a latter section, a case study is presented to examine the difference in results when continuous variables are considered, as against two sample sets of integer solutions. In light of this, it may be mentioned that although Mixed-Integer Nonlinear Programming (MINLP) problems can be solved using various heuristic methods, the difference might not be very significant as suggested, for example, in [31], wherein an OPF for various load conditions with discrete and continuous taps of LTCs is shown to produce similar results.

### A. Scenario 1: Uncontrolled Price-Responsive Loads

In this scenario, it is assumed that the customers respond to electricity prices as per the price-responsive load models introduced in Section III-B, and seek to reduce their energy cost as much as possible over the day, with all customers being equipped with HEMS that has access to a 24-hour price forecast. Based on this information, customers respond to electricity prices by deferring or interrupting some of their loads, without regard for system conditions. The LDC thus receives a revised load profile based on which it optimally determines the tap and capacitor operation schedule to maintain voltages and currents within prescribed limits.

Two different objective functions are considered within this scenario, minimization of $J_1$ and $J_2$ given by (21) and (23), respectively. For the linear price-responsive load model, the demand can be calculated using (10) to (13), and for the exponential price-responsive load, the demand is calculated using (11), (14), and (15). The 3-phase distribution feeder and its components, modeled by (1) to (7), and the network equations (8) and (9), are the constraints of the controlled system operational model, with variable taps and capacitors. The operating limits for this scenario are given by (25) to (28).

### B. Scenario 2: LDC Controlled Loads

In this mode of operation, it is assumed that the LDC incorporates a peak demand constraint within its DOPF program and the controllable/dispatchable component of the load ($\alpha_1$) is a variable which is optimally scheduled by the DOPF for customers. The objective functions considered here, minimization of $J_1$ and $J_2$, are from the LDC's perspective and are discussed in (21) and (23), while the third objective of minimization of $J_3$ is from the customers' perspective (24), as discussed earlier. The 3-phase distribution feeder and its components (1) to (7), network equations (9) and (20), and the constant energy model given by (16) to (19) are the constraints of the DOPF in this scenario. Additional operating constraints include limits on tap operation, capacitor switching, voltage and feeder current limits as discussed in (25) to (28). Note that no direct interruptible component is assumed in these controllable loads, and hence the issue of cold load pick-up or load recovery characteristics is not considered in the models used.

It should be noted that price elasticity matrices can also be used to determine the lateral movement of loads across time in response to prices; however, these models are not implemented in this paper, since a constant energy model is proposed instead to determine optimal load shifting. In this context, the controllable loads become variables to optimally compute their lateral shifting subject to grid constraints; hence,

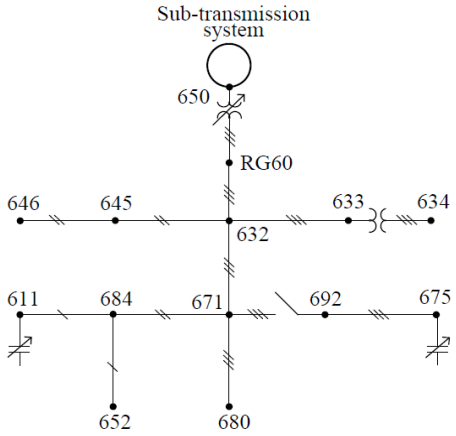


Fig. 5. IEEE 13-node test feeder [32].

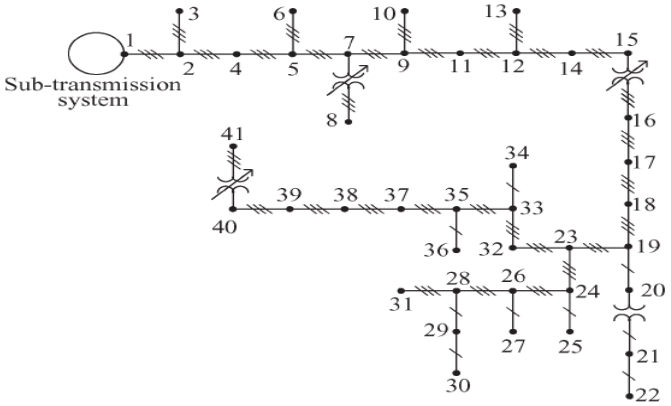


Fig. 6. Realistic LDC feeder [24].

price elasticity matrix models would effectively be variables which would be determined simultaneously (and optimally) from the model, based on the energy price and grid conditions.

## V. Results and Analysis

The proposed new DOPF models are validated on the IEEE 13-node test feeder (Fig. 5) [32], and a realistic distribution feeder (Fig. 6) [24]. For the 13-node feeder, the capacitors are modeled as multiple capacitor banks with switching options. For example, the capacitor at Bus 675 (Fig. 5) is assumed to comprise 5 blocks of 100 kVAr capacitors in each phase, and Bus 611 to have 5 blocks of 50 kVAr capacitors in phase $c$.

The practical LDC feeder system has three three-phase transformers equipped with LTCs and a single phase transformer. There are 16 load nodes, with all loads modeled as constant impedances. The feeder current limit information is not available in this case; hence, constraint (26) is not included in the DOPF models. A 24 hour base load profile is generated using the procedure discussed in [24].

In Ontario, the Hourly Ontario Electricity Price (HOEP) is calculated every hour and can be considered an RTP, that applies to customers participating in the wholesale electricity market [33]. The HOEP is therefore used for the analysis

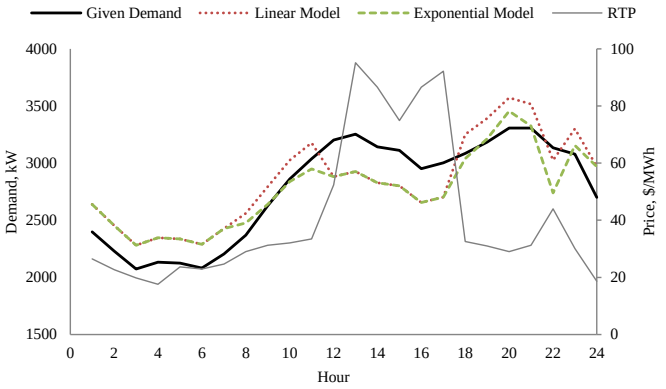


Fig. 7. System load profiles for uncontrolled price-responsive loads.

reported in this paper for a specific weekday of June 30, 2011. The Scenario 1 case studies are carried out assuming $\alpha$ = 0.20 (20% of the load is price-responsive) while Scenario 2 assumes that the share of controllable/dispatchable loads ($\alpha_1$) is 0.20. Customer defined constants for the first category of the load model are assumed to be: $\beta_1$ = 0.5, and $\beta_2$ = 1.5. For the exponential price-responsive model, the decay constant is assumed to be $\gamma$ = 0.8. Voltages are maintained within $\pm$5% for both Scenarios 1 and 2.

### A. IEEE 13-node Feeder

*1) Scenario 1: Uncontrolled Price-Responsive Loads:* Figure 7 shows the system load profile for linear and exponential price-responsive load models, compared with the base load. It is observed that the load decreases when the price is high, from 1-5 PM and also at 10 PM, as compared to the base load profile. Increase in the demand is observed when prices are low in the early morning and late evening hours. Note that the linear model is more sensitive to price signals as compared to the exponential model and the increase or decrease in demand is more, for the same prices.

Table I presents the summary results of LDC operation with base load (100% load is fixed), and for linear and exponential price-responsive load models considering minimization of $J_1$ and $J_2$. For the base load operation of LDC, the demand is considered to be non-responsive to prices, and taps and capacitors are considered variables. Note that there is an overall reduction in the cost of energy drawn by the LDC and the customers' energy cost when the loads are price-responsive, be it linear or exponential function. This indicates that the deployment of smart energy management devices in the distribution feeders could be advantageous for both parties. The energy drawn and feeder losses increase when loads are linearly price-responsive, but decrease when loads are exponentially price-responsive, which can be attributed to the price-demand relationships in each case and the associated parameters of the price-responsive models.

Since demand increases at low price hours in the late evening and early morning for price-responsive loads, the voltage profiles obtained from a distribution load flow (DLF) with fixed taps and capacitor banks, are lower than that for base load

TABLE I
SUMMARY RESULTS FOR SCENARIO 1 FOR IEEE 13 NODE FEEDER

| | | Total energy drawn by LDC [kWh] | Total feeder loss [kWh] | Total cost of energy drawn by LDC [$] | Total energy cost to customers [$] |
|---|---|---|---|---|---|
| Base Load | $J_1$ | 62,967 | 1,524 | 2,733 | 2,665 |
| | $J_2$ | 63,060 | 1,512 | 2,736 | 2,668 |
| Linear Load | $J_1$ | 64,487 | 1,583 | 2,667 | 2,602 |
| | $J_2$ | 64,577 | 1,573 | 2,670 | 2,605 |
| Exponential Load | $J_1$ | 62,667 | 1,493 | 2,607 | 2,544 |
| | $J_2$ | 62,763 | 1484 | 2,610 | 2,548 |

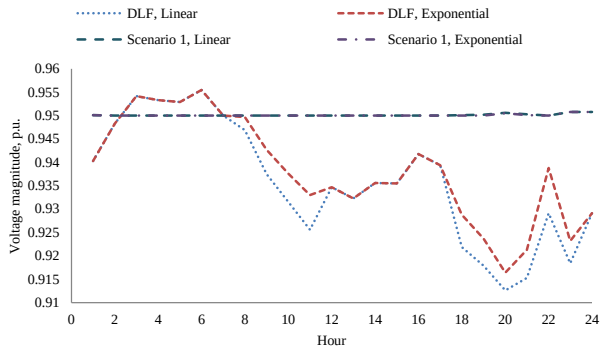


Fig. 8. Voltage magnitude at Node 675 in phase $c$ for Scenario 1.

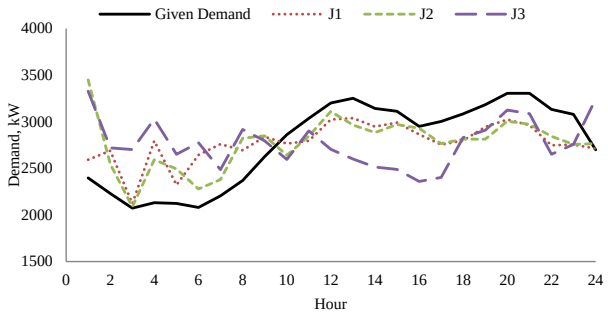


Fig. 9. System load profiles for LDC controlled loads.

($\alpha$=0). On the other hand, when the price-responsive demand falls during peak-price hours, the corresponding voltage profile from a DLF is better than that for the base load case. A comparison of the voltage profile at Node 675 in phase $c$ with and without tap and capacitor control (Fig. 8), shows that, a proper voltage profile within stipulated limits can be attained through controlled tap and capacitor switching operations.

*2) Scenario 2: LDC Controlled Loads:* Figure 9 presents the resulting system load profile when the LDC schedules the controllable/dispatchable portion of the loads, considering minimization of $J_1$, $J_2$, and $J_3$. It is to be noted that in this scenario the LDC imposes a peak demand constraint (19) in the system to ensure that no new peaks are created when there is load shifting across hours. The system load profiles are observed to be very similar for $J_1$ and $J_2$, and the demand decreases as compared to the base case between 1 PM to midnight, and increases during the early morning hours, illustrating a shift of the loads within the 24 hour period, with the same energy consumption over the day. Although a new peak is created at 1 AM with $J_2$, this is still within the LDC's prescribed peak demand constraint. Minimization of $J_3$ results in significant shifting of demand from afternoon and evening hours to early morning hours, since electricity prices are cheaper at these hours; this results in almost a flat load profile, which is desirable for the LDC. Thus, the use of $J_3$ by the LDC as an objective function for dispatching the controllable loads benefits both the LDC and customers.

The effect of varying the peak demand constraint is examined now, together with the minimum level of the peak demand constraint that the system can handle. This case study is carried out considering $J_1$ only. Figure 10 presents the effect

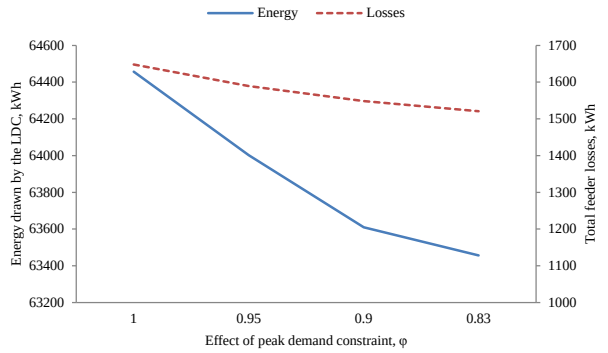


Fig. 10. Effect of peak demand constraint on LDC energy drawn and feeder losses.

of variation of the peak demand constraint ($\varphi$ is reduced from 1.0 to 0.83) on the energy drawn by the LDC and feeder losses. Note that as $\varphi$ decreases, i.e., the peak demand is reduced, the LDC draws less energy, feeder losses reduce, and consequently, its cost of energy drawn (Fig. 11) as well as the customers' cost of energy also decrease.

The minimum peak demand constraint that the system can sustain without requiring any load curtailment is $\varphi$ = 0.83; the system load profile for this case is presented in Fig. 12. Observe that the system load profile is evenly distributed over 24 hours.

*3) Uncertainty Analysis:* The analysis presented in Section VI.A.1 models the price-responsive loads with a selected set of parameters ($m$ and $\gamma$), which are highly unpredictable and difficult to estimate. Hence Monte Carlo simulations are carried out in this section considering uncontrolled price-responsive loads (Scenario 1) and minimization of $J_1$, with

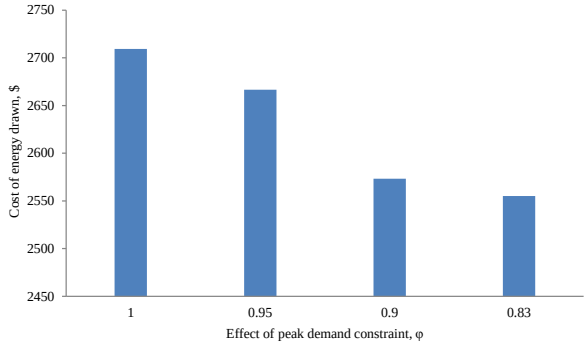


Fig. 11. Effect of peak demand constraint on cost of LDC energy drawn.

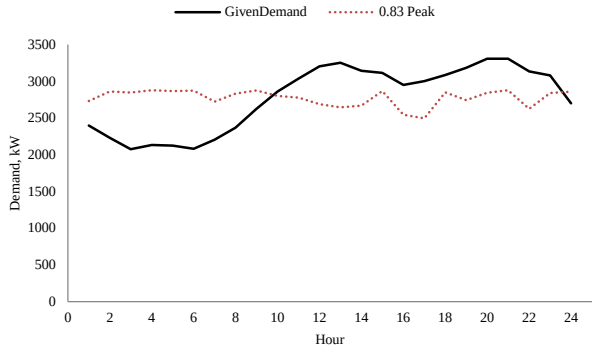


Fig. 12. System load profile for $\varphi$ = 0.83, $J_1$.

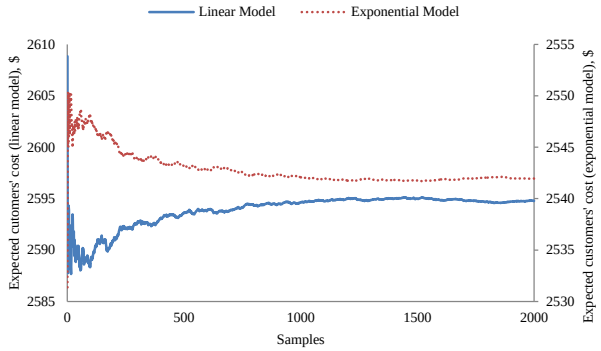


Fig. 13. Monte Carlo simulation of price-responsive loads.

TABLE II
MODEL PARAMETER HOURLY UNCERTAINTIES IN SCENARIO 1

| Case Studies | Linear Model | Exponential Model |
|---|---|---|
| Expected total energy drawn by LDC [kWh] | 64,494 | 62,570 |
| Expected total feeder losses [kWh] | 1,584 | 1,491 |
| Expected total LDC cost [$] | 2,668 | 2,603 |
| Expected total energy cost to customers [$] | 2,602 | 2,541 |

electricity price and parameters of the price-responsive load models considered uncertain.

Figure 13 presents the Monte Carlo simulation results for the linear and exponential price-responsive load models. In the linear price-responsive load model, the slope $m_{L,p,k}$ given by (12)-(13) is varied considering the price to be uniformly distributed in the range of $\pm 15$ \$/MWh with respect to its nominal value. For the exponential price-responsive load model, the decay parameter $\gamma$, representing the sensitivity of customers to prices, is varied using a uniform distribution in a range of 0.05 to 0.12. The simulations are performed for 2000 samples, since the expected energy cost converges after about 1000 sample runs. The resulting expected energy cost is \$2,595 and \$2,542 for the linear and exponential price-responsive load models, respectively. These expected values are very close to those obtained for a specific set of chosen parameters (Table I).

*4) Variability of Model Parameters Across Time:* The analysis presented so far assumes that $m$ and $\gamma$ remain unchanged for the entire 24 hour operation. However, this may not be the case in real-life, since, for example, a customer may reduce its load more at 10 AM, to the same price increase than it would do at 7 PM. Thus, to represent the variability of the elasticity parameters across time, Monte Carlo simulations are carried out here considering uncontrolled price-responsive loads and minimization of $J_1$; in this case, random sample sets are generated simultaneously for 24-hourly $m$ or $\gamma$. For the linear price-responsive load model, the slope $m_{L,p,k}$ given by (12)-(13) is varied hourly considering a uniform distribution in the range of $0.7m_{L,p,k}$ to $1.3m_{L,p,k}$. For the exponential price-responsive load model, $\gamma$ is varied hourly using a uniform distribution in the range of 0.05 to 0.12. The simulations are performed for 2000 samples.

Table II presents the expected values of solution outputs, i.e., energy drawn by LDC, feeder losses, cost of energy drawn by LDC, and energy cost to customers. Observe that the expected values are very close to those obtained in the deterministic case (Table I).

Figures 14 and 15 show four different plots of probability distributions of the solution outputs for linear and exponential price-responsive load models, respectively. These probability distributions depict the range of values over which the system variables are expected to vary hourly, for the assumed uniformly distributed parameters $m$ and $\gamma$. These plots depict narrow variations around the mean, thus showing that the deterministic studies discussed earlier are reasonable, since the results are close to the expected trends for the assumed model parameters.

*5) Differences in Continuous Versus Discrete Modeling:* The analyses reported thus far, consider the taps and capacitors to be continuous variables. Therefore, in this section, the following simple approach is used to examine the difference in the results when these are modeled as discrete variables:

1) The modified DOPF is executed with taps and capacitors as continuous variables.
2) The optimal solutions of the continuous variables $T_{t,p,k}$ and $cap_{C,p,k}$ from Step 1 are rounded-up (RUp) and rounded-down (RDn) to the nearest discrete values.
3) The proposed DOPF is then run for all possible combinations of RUp and RDn values of taps and capacitors to obtain the "outlier" solutions associated with the corresponding discrete values.

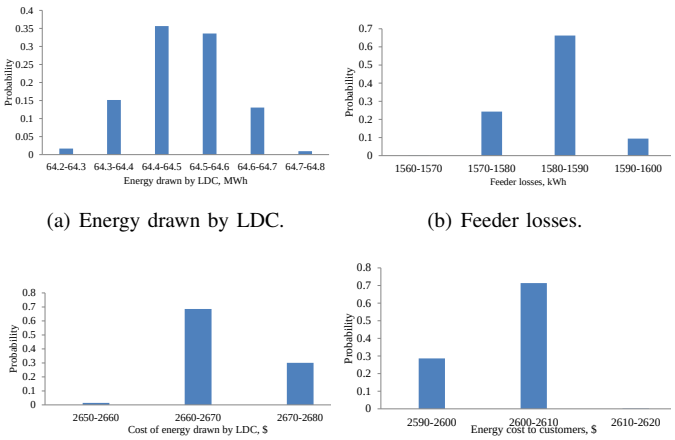


(a) Energy drawn by LDC. (b) Feeder losses.

(c) Cost of energy drawn by LDC. (d) Energy cost to customers.

Fig. 14. Probability distribution of solution outputs for linear price-responsive loads.

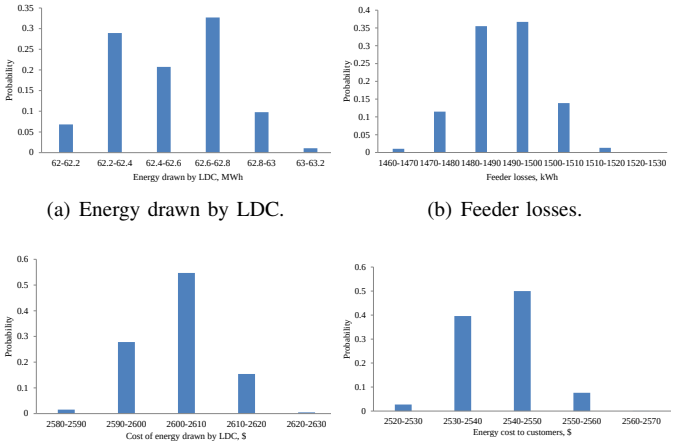


(a) Energy drawn by LDC. (b) Feeder losses.

(c) Cost of energy drawn by LDC. (d) Energy cost to customers.

Fig. 15. Probability distribution of solution outputs for exponential price-responsive loads.

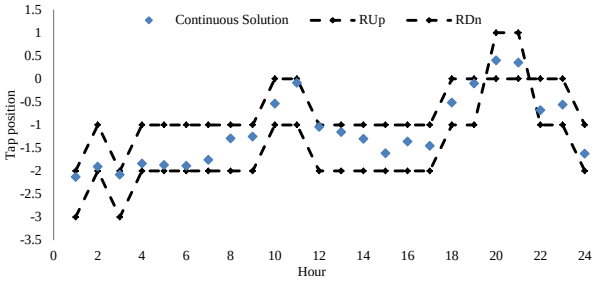


Fig. 16. Continuous optimal $T_{650}$ and its corresponding RUp and RDn values.

TABLE III
POSSIBLE DISCRETE COMBINATIONS OF TAP AND CAPACITOR VALUES

| | $T_{650}$ | $cap_{675}$ | $cap_{611}$ |
|---|---|---|---|
| Outlier 1 | RUp | RUp | RUp |
| Outlier 2 | RUp | RUp | RDn |
| Outlier 3 | RUp | RDn | RUp |
| Outlier 4 | RUp | RDn | RDn |
| Outlier 5 | RDn | RUp | RUp |
| Outlier 6 | RDn | RUp | RDn |
| Outlier 7 | RDn | RDn | RUp |
| Outlier 8 | RDn | RDn | RDn |

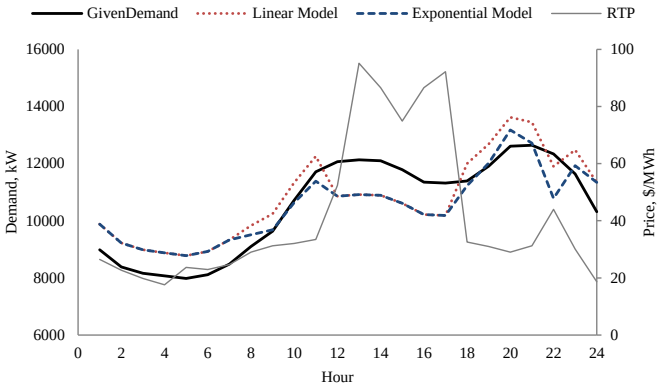


Fig. 17. System load profile for uncontrolled mode for a realistic LDC feeder.

The aforementioned approach is applied to the uncontrolled price-responsive loads for the minimization of $J_1$. Figure 16 illustrates the continuous solution and the RUp and RDn integer values for $T_{t,p,k}$ only, for the linear price-responsive load model. All the possible combinations obtained from the RUp and RDn values are shown in Table III, and all the possible outlier DOPF solutions for the linear price-responsive load model are presented in Table IV. Notice that the solution differences are minimal for the continuous versus the discrete values. Similar results were obtained for the exponential price-responsive load model.

### B. Realistic LDC Feeder

*1) Scenario 1: Uncontrolled Price-Responsive Loads:* Studies are carried out considering a practical LDC feeder with linear and exponential price-responsive load models. The resulting system load profiles with these models, as presented in Fig. 17, are very similar to those obtained for the IEEE 13-node test feeder, with the linear model being more sensitive to price signals as compared to the exponential. The demand decreases when the price is high (between 1 to 5 PM) and increases when low (early morning and late evenings).

Table V presents the main results of LDC's operation for the base load case, and with the linear and exponential price-responsive load models considering minimization of $J_1$ and $J_2$. Observe that the price-responsive load models result in reduced cost of energy drawn by the LDC and energy cost to customers as compared to the base load case, a desirable result for both the LDC and customers.

*2) Scenario 2: LDC Controlled Loads:* Figure 18 presents a comparison of the system load profiles obtained considering minimization of $J_1$, $J_2$, and $J_3$, for the controlled load profiles vis-a-vis the base load profile. Note that the controlled load profiles using $J_1$ and $J_2$ are very similar, i.e., the load decreases from afternoon onwards to midnight, shifting it to early morning hours and resulting in a more uniform profile.

TABLE IV
CONTINUOUS AND DISCRETE DOPF SOLUTION FOR LINEAR PRICE-RESPONSIVE MODEL

| | Continuous | Outlier 1 (Dif. %) | Outlier 2 (Dif. %) | Outlier 3 (Dif. %) | Outlier 4 (Dif. %) | Outlier 5 (Dif. %) | Outlier 6 (Dif. %) | Outlier 7 (Dif. %) | Outlier 8 (Dif. %) |
|---|---|---|---|---|---|---|---|---|---|
| Total Energy drawn by LDC [kWh] | 64,487 | 64,517 (0.046) | 64,495 (0.012) | 63,769 (-1.114) | 63,749 (-1.145) | 65,162 (1.047) | 65,141 (1.013) | 64,406 (-0.126) | 64,386 (-0.157) |
| Total feeder losses [kWh] | 1,583 | 1,586 (0.186) | 1,585 (0.153) | 1,577 (-0.349) | 1,577 (-0.342) | 1,601 (1.132) | 1600 (1.1) | 1,592 (0.594) | 1,592 (0.601) |
| Total LDC cost [$] | 2,667 | 2,667 (-0.031) | 2,666 (-0.049) | 2,635 (-1.232) | 2,634 (-1.25) | 2,695 (1.042) | 2,695 (1.024) | 2,663 (-0.173) | 2,662 (-0.191) |
| Total energy cost to customers [$] | 2,602 | 2,601 (-0.036) | 2,601 (-0.055) | 2,570 (-1.249) | 2,569 (-1.267) | 2,629 (1.038) | 2,629 (1.019) | 2,597 (-0.189) | 2,597 (-0.207) |

TABLE V
RESULTS FOR SCENARIO 1 FOR A REALISTIC LDC FEEDER

| | | Total energy drawn by LDC [kWh] | Total feeder loss [kWh] | Total cost of energy drawn by LDC [$] | Total energy cost to customers [$] |
|---|---|---|---|---|---|
| Base Load | $J_1$ | 244 | 3.835 | 10,552 | 10,379 |
| | $J_2$ | 246 | 3.825 | 10,670 | 10,497 |
| Linear Load | $J_1$ | 250 | 3.997 | 10,317 | 10,153 |
| | $J_2$ | 252 | 3.987 | 10,427 | 10,263 |
| Exponential Load | $J_1$ | 243 | 3.753 | 10,096 | 9,940 |
| | $J_2$ | 246 | 3.744 | 10,206 | 10,050 |

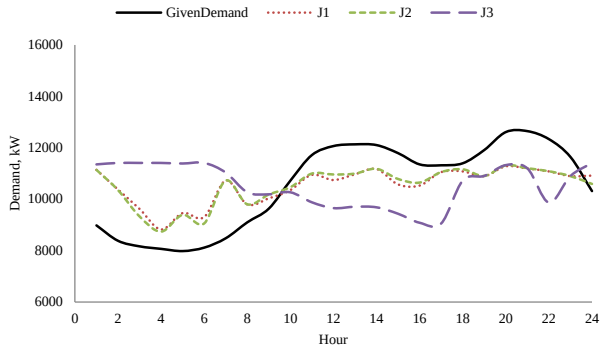


Fig. 18. System load profile considering $J_1$, $J_2$ and $J_3$ for a realistic LDC feeder.

TABLE VI
RESULTS FOR CONTROLLED LOADS FOR SCENARIO 2 FOR A REALISTIC LDC FEEDER

| Case Studies | $J_1$ | $J_2$ | $J_3$ |
|---|---|---|---|
| Total Energy drawn by LDC [MWh] | 245 | 248 | 251 |
| Total feeder losses [MWh] | 3.792 | 3.773 | 4.114 |
| Total LDC cost [$] | 10,091 | 10,267 | 10163 |
| Controllable customers' cost [$] | 1,669 | 1,711 | 1,450 |

TABLE VII
COMPUTATIONAL STATISTICS

| | IEEE 13-node test feeder | | Real distribution feeder | |
|---|---|---|---|---|
| | Price-responsive | Controllable load | Price-responsive | Controllable load |
| No. of Equations | 21,914 | 26,155 | 56,199 | 65,459 |
| No. of Variables | 21,026 | 25,250 | 54,003 | 63,194 |
| Execution time [s] | 0.141 | 3.089 | 2.452 | 1.046 |

Minimization of $J_3$ and peak demand constraint results in a fairly flat but elevated load profile at early morning hours.

Table VI presents a comparison of the LDC controlled cases considering minimization of $J_1$, $J_2$, and $J_3$. Observe that minimization of $J_1$ results in the lowest energy drawn by the LDC, while the customers' cost pertaining to the variable component of the load is lowest when $J_3$ is minimized, although feeder losses increase when compared to minimization of $J_1$ and $J_2$. Finally, note that the overall operational trends for a realistic LDC feeder are similar to those obtained for the IEEE 13-node test feeder.

### C. Modeling, Algorithm and Computational Challenges

The proposed DOPF model has been programmed and executed on a Dell PowerEdge R810 server, in the GAMS environment [34], Windows 64-bit operating system, with 4 Intel Xeon 1.87 GHz processors and 64 GB of RAM. The mathematical model is an NLP problem which is solved using the SNOPT solver [34]. The model and solver statistics for the IEEE 13-node test feeder and the real distribution feeder are summarized in Table VII.

Some of the modeling, algorithmic, and computational challenges of the proposed approach are the following:

- There is a need for real-time data from customer loads, measured through smart meters, to accurately estimate the parameters using the proposed SLE for the price-responsive load models.
- Modeling of controllable loads introduces sine and cosine functions in the load representation, which increase the model complexity.
- With the introduction of controllable loads, the number of equations and variables increase as compared to price-responsive loads, and introduces inter-temporal constraints in the NLP optimization problem, which make

it more challenging to solve.

- As shown in Table VII, the size and complexity of the proposed DOPF problem, is quite significant, but the execution times are quite reasonable and appropriate for the proposed real-time applications.

## VI. Conclusions

This paper proposed two representations of customer load models in the context of smart grids, integrating them within an unbalanced distribution system operational framework. In the first model, uncontrolled price-responsive load models were formulated, considering that these respond to price signals either linearly or in an exponential manner. The resulting load profile was used by the LDC to determine the impact on feeder operations. The second model assumes LDC controlled, constant energy loads, which could be shifted across intervals.

A novel operational framework from the LDC's perspective was developed, ensuring that no new peak is created in the system, while smart loads are optimally shifted. Various case studies were considered from the perspective of both the LDC and customers and tested on realistic feeders, considering uncertainty on the price-responsive load parameters. The controlled load model resulted in a more uniform system load profile with respect to uncontrolled loads, and a peak demand cap led to decrease in energy drawn as the cap was reduced, consequently reducing feeder losses and LDC's and customers' costs.

## References


[1] "FERC Staff Report: Assesment of Demand Response and Advanced Metering," Dec. 2012. [Online]. Available: http://www.ferc.gov/legal/staff-reports/12-20-12-demand-response.pdf

[2] A. Sanghvi, "Flexible strategies for load/demand management using dynamic pricing," *IEEE Trans. Power Syst.*, vol. 4, no. 1, pp. 83–93, Feb 1989.

[3] F. Schweppe, R. Tabors, J. Kirtley, H. Outhred, F. Pickel, and A. Cox, "Homeostatic utility control," *IEEE Trans. Power App. and Syst.*, vol. PAS-99, no. 3, pp. 1151–1163, May 1980.

[4] EPRI, "EPRI Innovative Rate Design Study," Jan. 1985.

[5] P. Jazayeri, A. Schellenberg, W. D. Rosehart, J. Doudna, S. Widergren, D. Lawrence, J. Mickey, and S. Jones, "A survey of load control programs for price and system stability," *IEEE Trans. Power Syst.*, vol. 20, no. 3, pp. 1504–1509, Aug 2005.

[6] A. David and Y. C. Lee, "Dynamic tariffs: theory of utility-consumer interaction," *IEEE Trans. Power Syst.*, vol. 4, no. 3, pp. 904–911, Aug 1989.

[7] K. Bhattacharya, M. Bollen, and J. Daalder, "Real time optimal interruptible tariff mechanism incorporating utility-customer interactions," *IEEE Trans. Power Syst.*, vol. 15, no. 2, pp. 700–706, May 2000.

[8] D. Kirschen, G. Strbac, P. Cumperayot, and D. de Paiva Mendes, "Factoring the elasticity of demand in electricity prices," *IEEE Trans. Power Syst.*, vol. 15, no. 2, pp. 612–617, May 2000.

[9] E. Bompard, Y. Ma, R. Napoli, and G. Abrate, "The demand elasticity impacts on the strategic bidding behavior of the electricity producers," *IEEE Trans. Power Syst.*, vol. 22, no. 1, pp. 188–197, Feb 2007.

[10] "Demand response modeling considering interruptible/curtailable loads and capacity market programs," *Applied Energy*, vol. 87, no. 1, pp. 243 – 250, 2010.

[11] A. Khodaei, M. Shahidehpour, and S. Bahramirad, "SCUC with hourly demand response considering intertemporal load characteristics," *IEEE Trans. Smart Grid*, vol. 2, no. 3, pp. 564–571, Sept 2011.

[12] A. Abdollahi, M. Moghaddam, M. Rashidinejad, and M. Sheikh-El-Eslami, "Investigation of economic and environmental-driven demand response measures incorporating uc," *IEEE Trans. Smart Grid*, vol. 3, no. 1, pp. 12–25, March 2012.

[13] K. Dietrich, J. Latorre, L. Olmos, and A. Ramos, "Demand response in an isolated system with high wind integration," *IEEE Trans. Power Syst.*, vol. 27, no. 1, pp. 20–29, Feb 2012.

[14] J. Aghaei and M.-I. Alizadeh, "Critical peak pricing with load control demand response program in unit commitment problem," *IET Generation, Transmission Distribution*, vol. 7, no. 7, pp. 681–690, July 2013.

[15] C. De Jonghe, B. Hobbs, and R. Belmans, "Optimal generation mix with short-term demand response and wind penetration," *IEEE Trans. Power Syst.*, vol. 27, no. 2, pp. 830–839, May 2012.

[16] A. Safdarian, M. Fotuhi-Firuzabad, and M. Lehtonen, "Benefits of demand response on operation of distribution networks: A case study," *IEEE Systems Journal*, Early Access Article 2014.

[17] K. Tanaka, K. Uchida, K. Ogimi, T. Goya, A. Yona, T. Senjy, T. Funabashi, and C.-H. Kim, "Optimal operation by controllable loads based on smart grid topology considering insolation forecasted error," *IEEE Trans. Power Syst.*, vol. 2, no. 3, pp. 438–444, Sept. 2011.

[18] H. Jorge, C. Antunes, and A. Martins, "A multiple objective decision support model for the selection of remote load control strategies," *IEEE Trans. Power Syst.*, vol. 15, no. 2, pp. 865–872, May 2000.

[19] C. Kurucz, D. Brandt, and S. Sim, "A linear programming model for reducing system peak through customer load control programs," *IEEE Trans. Power Syst.*, vol. 11, no. 4, pp. 1817–1824, Nov. 1996.

[20] H. Saele and O. Grande, "Demand response from household customers: experiences from a pilot study in Norway," *IEEE Trans. Smart Grid*, vol. 2, no. 1, pp. 102–109, March 2011.

[21] A. Conejo, J. Morales, and L. Baringo, "Real-time demand response model," *IEEE Trans. Smart Grid*, vol. 1, no. 3, pp. 236–242, Dec. 2010.

[22] S. Shao, M. Pipattanasomporn, and S. Rahman, "Demand response as a load shaping tool in an intelligent grid with electric vehicles," *IEEE Trans. Smart Grid*, vol. 2, no. 4, pp. 624–631, Dec. 2011.

[23] M. Bozchalui, S. Hashmi, H. Hassen, C. Cañizares, and K. Bhattacharya, "Optimal operation of residential energy hubs in smart grids," *IEEE Trans. Smart Grid*, vol. 3, no. 4, pp. 1755–1766, Dec 2012.

[24] S. Paudyal, C. Cañizares, and K. Bhattacharya, "Optimal operation of distribution feeders in smart grids," *IEEE Trans. Ind. Electron*, vol. 58, no. 10, pp. 4495–4503, Oct. 2011.

[25] P. Palensky and D. Dietrich, "Demand side management: Demand response, intelligent energy systems, and smart loads," *IEEE Trans. Ind. Informat*, vol. 7, no. 3, pp. 381–388, Aug 2011.

[26] "US Department of Energy." [Online]. Available: http://energy.gov/oe/technology-development/smart-grid

[27] W. H. Kersting, *Distribution System Modeling and Analysis*, 2nd ed. CRC Press, 2006.

[28] C. Chen, J. Wang, Y. Heo, and S. Kishore, "MPC-based appliance scheduling for residential building energy management controller," *IEEE Trans. Smart Grid*, vol. 4, no. 3, pp. 1401–1410, Sept 2013.

[29] F. Ramos, C. A. Cañizares, and K. Bhattacharya, "Effect of price responsive demand on the operation of microgrids," *Proc. Power Systems Computation Conference*, August 2014.

[30] "Peaksaver Plus Program." [Online]. Available: http://www.hydroone.com/MyHome/SaveEnergy/Pages/Peaksaver.aspx

[31] A. Papalexopoulos, C. F. Imparato, and F. Wu, "Large-scale optimal power flow: effects of initialization, decoupling and discretization," *IEEE Trans. Power Syst.*, vol. 4, no. 2, pp. 748–759, May 1989.

[32] W. H. Kersting, "Radial distribution test feeders," in *2001 IEEE Power Engineering Society Winter Meeting*, vol. 2, 2001, pp. 908 –912.

[33] "IESO." [Online]. Available: http://www.ieso.ca/imoweb/marketdata/hoep.asp

[34] "GAMS Solver Description." [Online]. Available: http://www.gams.com/solvers/solvers.htm


**Isha Sharma** (S'09) received the Bachelors degree in Electrical and Computer Engineering from the University of Windsor, Windsor, Ontario, Canada in 2009. She is currently working toward the Ph.D. degree in Electrical Engineering at the University of Waterloo, Waterloo, ON, Canada. Her research interests are in distribution system modeling and analysis in the context of Smart Grids.

**Kankar Bhattacharya** (M'95 SM'01) received the Ph.D. degree in Electrical Engineering from the Indian Institute of Technology, New Delhi, India, in 1993. He was in the faculty of Indira Gandhi Institute of Development Research, Mumbai, India, during 1993-1998, and then the Department of Electric Power Engineering, Chalmers University of Technology, Gothenburg, Sweden, during 1998-2002. He joined the E&CE Department of the University of Waterloo, Waterloo, ON, Canada, in 2003 where he is currently a full Professor. His research interests are in power system economics and operational aspects.

**Claudio Cañizares** (S'85 M'91 SM'00 F'07) received the Electrical Engineer Diploma from the Escuela Politécnica Nacional (EPN), Quito, Ecuador, in April 1984, the M.S. and Ph.D. degrees in electrical engineering from the University of Wisconsin-Madison, in 1988 and 1991, respectively. He had held various academic and administrative positions at the E&CE Department of the University of Waterloo, Waterloo, ON, Canada, since 1993, where he is currently a full Professor, the Hydro One Endowed Chair, and the Associate Director of the Waterloo Institute for Sustainable Energy (WISE). His research interests are in modeling, simulation, control, stability, computational and dispatch issues in sustainable power and energy systems in the context of competitive markets and Smart Grids.